Desalination and Water Treatment
www.deswater.com
doi: 10.5004/dwt.2021.27562

241 (2021) 257–262
November

Study on the hydrochemical characteristics and formation mechanism of shallow salt water in the north of Jinan based on factor analysis

Chunhong Yuan[a,b,]*, Qingjie Yue[c]

[a]*801 Institute of Hydrogeology and Engineering Geology, Shandong Provincial Bureau of Geology & Mineral Resources, Shandong Jinan 250014, China, email: chunhongy912@163.com*
[b]*Shandong Engineering Research Center for Environmental Protection and Remediation on Groundwater Shandong Jinan 250014, China*
[c]*Jinan Bureau of Natural Resources and planning, Shandong Jinan 250001, China*

Received 25 June 2021; Accepted 23 September 2021

ABSTRACT

In order to study the hydrogeological characteristics and hydrochemical distribution characteristics of shallow saline water, the main factors that affect the hydrochemical field can be effectively identified. In this paper, the hydrochemical data of 85.302% shallow salt water in the study area were studied by factor analysis method, combined with the local hydrogeological conditions and hydrochemical type characteristics. The results show that the shallow salt water has undergone strong mixing and evaporation and concentration, and the contribution rates are 61.671% and 23.631%, respectively. The study is of great significance for improving and protecting the groundwater environment, enhancing the groundwater supply capacity, ensuring the water supply safety and promoting the sustainable development of the new urban area in the north area of Jinan.

Keywords: Factor analysis; Shallow salt water; Hydrochemical characteristics; North of Jinan

1. Introduction

Groundwater resource is an important resource guarantee for urban construction and development, which not only affects the daily life of local people, but also plays a vital role in the future development of cities. Jinan North Cross District is located in the north of Jinan City, located in the alluvial plain of the Yellow River, including Sangzidian Town and Daqiao Town in Tianqiao District and parts of Sungeng Town, Cuizhai Town, Huihe Town and Chengguan Town in Jiyang District. Shallow pore water is the main groundwater type in this area, which can be divided into fresh water, brackish water and brackish water according to the change and distribution of salinity and main chemical components on the plane. Total dissolved solids (TDS) greater than 3 g/L is saline water, TDS 2–3 g/L is brackish water, TDS less than 2 g/L is fresh water. The TDS of shallow pore water in the northern cross-region is generally 1–3 g/L, and the highest is 5.284 g/L, belonging to the distribution area of brackish water to brackish water. The area of Gaohuaijia–Dongyanchang–Houwubaodian–Jinjiazhuang is 85.57 km^2, and the TDS of shallow pore water is greater than 3 g/L, which is the salt water outburst area [1].

2. Literature review

The formation of groundwater is controlled by factors such as quaternary sedimentary environment, paleoclimate, lithofacies and paleogeography, geological structure and hydrogeological conditions. The hydrochemical

* Corresponding author.

1944-3994/1944-3986

characteristics of groundwater in the area are zoned in both horizontal and vertical directions. In the horizontal direction, from west to east, that is, along the decreasing direction of the hydraulic slope of ancient groundwater, the TDS content of groundwater gradually increased, and the hydrochemical types also changed accordingly; In the vertical direction, groundwater moves from bottom to top, from fresh water to salt water. Water flow is the carrier of salt transport. Therefore, in order to study the evolution model of hydrochemistry, it is necessary to first identify the circulation process of groundwater. At present, the methods used to study groundwater circulation mainly include hydrogeological condition analysis, hydrochemical method and environmental isotope method.

Li using isotope values and conventional indicators such as content in the water, water and confined water of law, explains the suxichang regional migration mechanism of shallow groundwater water cycle system, the results show that micro suxichang regional confined water of mining increases the micro pressure difference between the water and groundwater level, lead to micro confined water of pirate scuba diving, surface water, Divers, on the other hand, are directly fed by rainwater and can quickly recover during the rainy season after being raided [2]. Liu et al. [3] studied the groundwater circulation in the Cretaceous basin of Ordos by using the characteristics of different water isotopes. Prasad and Yadav [4] studied the recharge relationship between Heihe water and groundwater in the Heihe River Basin, and estimated the amount of water and groundwater transformation. Chacko et al. [5] studied the conversion relationship between different water bodies by comparing and analyzing the D and 18O characteristics of atmospheric precipitation, surface water and groundwater in Ordos Basin. By analyzing groundwater, water isotopes and hydrochemical indexes of the Yellow River, Sahana et al. [6] established the circulating model of middle-shallow and deep groundwater in Yinchuan Plain.

3. Background and conditions of regional geology and hydrogeology

3.1. Physical geography

This area is located in the alluvial plain of the Yellow River, the terrain is relatively flat, the ground slope is 0.1×10^{-3}–0.2×10^{-3}, the ground elevation is 16–20 m, tilting from southwest to northeast. The microgeomorphology type is crevice fan-shaped land and gentle slope land. According to the precipitation data from 1956 to 2018, the average annual precipitation is 703.43 mm, the maximum annual precipitation is 1,064.5 mm, and the minimum annual precipitation is 342.85 mm.

3.2. Regional geology

This area is located in the first class tectonic unit of the North China Block and the second class tectonic unit of the West Shandong Uplift. The strata belong to the North China Stratigraphic Region, Shin-Hebei-Shan-Henan Stratigraphic Region, and the West Shandong Stratigraphic Region. The regional distribution includes Quaternary, Neogene, Carboniferous, Permian and Ordovician.

3.3. Regional hydrogeology

According to the previous hydrogeological data, the pore water of loose rock in the north region can be divided into three basic types: shallow phreatic water–micro-confined water, middle confined water and deep confined water at 500 m. According to the vertical change and distribution of TDS and its main chemical components, it can be further divided into shallow fresh water, middle salty water and deep fresh water. TDS greater than 3 g/L is salt water, TDS 2–3 g/L is brackish water, and TDS less than 2 g/L is fresh water.

3.4. Hydrogeological conditions in the study area

The salt water in the study area is distributed in Gaohuaijia — Dongyanchang — Houwubaodian — Jinjiazhuang, covering an area of 85.57 km^2, with TDS greater than 3 g/L. The formation lithology is silty soil in the upper part and silty clay, clay and sand in the lower part (Fig. 1). No.20 borehole showed two layers of fine silty sand with a thickness of 1.20–2.10 m. No. 26 and No. 27 boreholes showed one layer of fine silty sand with a thickness of 3.70–6.20 m. The lithology is clay. The buried depth of roof is 4.30–5.00 m, the buried depth of floor is 11.20–14.00 m, the thickness is 2.00–8.60 m, and there is no continuous clay layer below 15 m. The buried depth of water level is 1–4 m, and the water abundance is greatly affected by the ancient channel. The water inflow of a single well in the ancient channel is 1,000–3,000 m^3/d, and the interzone and marginal zone of

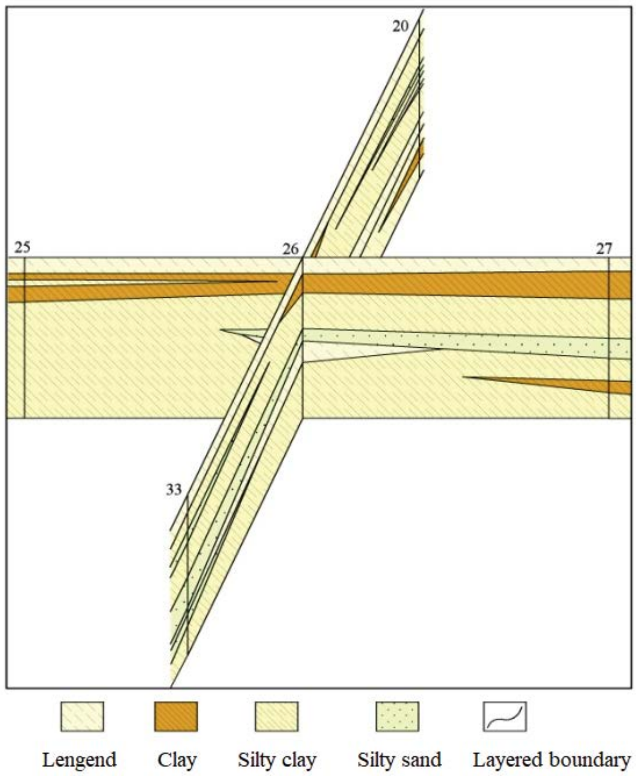

Fig. 1. Three-dimensional structure profile.

the ancient channel is less than 1,000 m^3/d. The water quality is poor, TDS3–5 g L of shallow groundwater, the anions are mostly SO_4·HCO_3·Cl, SO_4·Cl type, and the cations are mostly Na·Mg type. The area receives meteoric precipitation supply and Yellow River irrigation supply. Groundwater runoff from southwest to northeast, located in the groundwater runoff area; vertical evaporation is the main way of excretion.

4. Hydrochemical characteristics of salt water in the study area

4.1. Types of hydrochemistry

According to Shukarev classification, the anion hydrochemical types in the study area are SO_4·Cl, HCO_3·Cl·SO_4 and Cl type, SO_4·Cl is the main anion type in the study area, which is widely distributed in the middle of the study area; HCO_3·Cl·SO_4 is the secondary anion type in the study area, distributed in the northwest, southwest and southeast marginal zones of the SO_4·Cl distribution area; Cl was only distributed in Gaohuaijia-Dongyanchang area in the northeast corner of the study area.

There are two types of cationic water chemistry in the study area: Na·Mg·Ca and Na·Mg·Ca. Na·Mg·Ca water is widely distributed in the study area and is the main groundwater type. Na·Mg·Ca water is distributed in Sijiacun—Shuangmiao area in the southeast of the study area and has a small distribution area. Therefore, it can be seen that the chemical types of salt water are relatively complex [7].

4.2. TDS distribution

The distribution of TDS in Houbaodian was centered, and the distribution shape was an isosceles triangle from northwest to southeast. The TDS value was greater than 3 g/L, and the maximum value was 5.284 g/L in Houbaodian Village.

4.3. Distribution characteristics of chemical components

The concentration of Na^+ is basically centered in Zhangjiamiao, showing an elliptical distribution from southwest to northeast. The concentration is generally 400–800 mg/L, and the peak value is located at the gate of the first landfill plant (900.00 mg/L).

The concentration of Cl^- is distributed in a zonal direction from southwest to northeast with Jingzhuang — Houwubaodian — Zhanggongdian — Dongchang as the center. The concentration value is generally 400–800 mg/L, and the peak value is located in Dongchang (1,299.18 mg/L).

Ca^{2+} concentration value is generally 100–400 mg/L, Jingzhuang — Houwubaodian — Zhanggongdian line southeast Ca^{2+} concentration value 200–400 mg/L, the northwest line 100–200 mg/L.

The concentration of Mg^{2+} was centered in Dongyanchang — Houwubaodian — Sijiazhuang, with a general circular distribution, and the concentration was 200–400 mg/L.

The concentration value of SO_4^{2-} is centered in Dongchang — Houwubaodian — Jingzhuang — Sijiazhuang, and generally presents a heart-shaped distribution. The concentration value is generally 800–1,600mg/L, and the peak value is located in Houwubaodian (1,932.60 mg/L).

The concentration of HCO_3^- is generally 800–1,000 mg/L, and the peak value is located at the gate of the first landfill site (1,310.07 mg/L).

According to the above contour map of major ions, it can be concluded that the distribution law of major ion concentrations in the region is roughly consistent with that of TDS.

5. Formation mechanism research

5.1. Data Sources

In this study, 12 groups of salt water samples were used, and the analysis data included K^+, Na^+, Ca^{2+}, Mg^{2+}, SO_4^{2-}, Cl^-, HCO_3^-, total hardness, TDS, pH value and 11 trace elements test results.

5.2. Factor analysis

Factor analysis is a multivariate statistical analysis method with dimensionality reduction, that is, a few principal factors are used to replace the original more samples or variables, and these principal factors can reflect the information reflected by the original more samples or variables as much as possible, at the same time, they are independent of each other.

- Selection of original data

Choose the Na^+, Ca^{2+}, Mg^{2+}, Cl^-, SO_4^{2-}, HCO_3^-, TDS etc seven common groundwater chemical components were used as calculation variables and factor analysis was carried out in SPSS software. The original hydrochemical data matrix is as follows:

$$X = \begin{bmatrix} x_{11} & x_{12} & \cdots & x_{1p} \\ x_{21} & x_{22} & \cdots & x_{2p} \\ \vdots & \vdots & \vdots & \vdots \\ x_{n1} & x_{n2} & \cdots & x_{np} \end{bmatrix} \quad (1)$$

However, figuring out the underlying rules in so many variables is tricky. In order to overcome the complexity of analyzing data in P-dimensional space, dimensionality reduction is needed. Several independent comprehensive indexes are selected to replace the original many variable indexes, and at the same time, they can better reflect the information reflected by the original many indexes. The mathematical model is as follows:

$$\begin{cases} x_1 = a_{11}F_1 + a_{12}F_2 + \cdots + a_{1m}F_m + a_1\varepsilon_1 \\ x_2 = a_{21}F_1 + a_{22}F_2 + \cdots + a_{2m}F_m + a_2\varepsilon_2 \\ \cdots \\ x_p = a_{p1}F_1 + a_{p2}F_2 + \cdots + a_{pm}F_m + a_p\varepsilon_p \end{cases} \quad (2)$$

where x_i is the ith initial variable (i = 1, 2, … p); F_j is the factor variable (j = 1, 2, … m, $m < p$); a_{ij} is the factor loading; ε is the special factor

Factor load a_{ij} is a correlation coefficient reflecting the relative importance of x_i on the jth common factor variable.

Therefore, the greater the absolute value of a_{ij}, the stronger the relationship between the factor variable F_j and the original variable x_i.

- Standardized processing of original data

Due to the large concentration differences between the monitoring data, the original monitoring data are standardized to eliminate the effects of order of magnitude or dimension.

$$x_{ij}^* = \frac{x_{ij} - \bar{x}_j}{S_{ij}} \tag{3}$$

$$S_{ij} = \frac{1}{n}\sum_{k=1}^{n}\left(x_{ki} - \bar{x}_i\right)\left(x_{ij} - \bar{x}_j\right) \tag{4}$$

where i = 1, 2, …, n, n is the total number of samples; j = 1, 2, …, p, p is the number of initial variables in the sample; x_{ij}* is the standardized hydrochemical data.

Thus, the standard matrix $[x_{ij}]_{n\times p}$ of the raw water chemical data matrix is obtained. For convenience, it is still denoised as:

$[x_{ij}^*]_{n\times p} = [x_{ij}]_{n\times p}$

- Correlation coefficient matrix R of $[x_{ij}]_{n\times p}$ for calculated data:

$$r_{ij} = \frac{\sum_{n=1}^{n}\left(x_i - \bar{x}\right)\sum_{j=1}^{n}\left(y_i - \bar{y}\right)}{\sqrt{\sum_{i=1}^{n}\left(x_i - \bar{x}\right)^2\sum_{j=1}^{n}\left(y_i - \bar{y}\right)^2}} \tag{5}$$

The larger the absolute value of the correlation coefficient is, the stronger the correlation is; The smaller the absolute value is, the weaker the correlation is. The value of correlation strength is shown in Table 1.

- Calculate m eigenvalues and eigenvectors of R

Eigenvalue equation of the | | lambda $I - R = 0$ characteristic value λ_i (i = 1, 2, …, m) find them and arrange them in order of magnitude, that is $\lambda_1 \geq \lambda_2 \geq \ldots \geq \lambda_m > 0$; Then the eigenvectors u_1, u_2 … corresponding to the eigenvalue λ_1 are obtained, u_m, they are orthonormal [8].

- Calculate the contribution rate of the factor variable and the cumulative contribution rate Q

$$Q = \sum_{j=1}^{k}\frac{\lambda_j}{\sum_{i=1}^{m}\lambda_i} \tag{6}$$

$k \leq m$

The contribution rate of each factor variable is:

$$\frac{\lambda_i}{\sum_{i=1}^{m}\lambda_i}\left(i = 1, 2, \cdots, m\right) \tag{7}$$

The eigenvalues λ_1, λ_2, … are taken as the characteristic values whose cumulative contribution rate reaches over 80%. λ_m corresponds to the first, second…, the $m(m \leq p)$ factor variable.

Table 1
Correlation grading table

Highly relevant	0.8–1.0
Strong correlation	0.6–0.8
Moderate correlation	0.4–0.6
Weak correlation	0.2–0.4
Absence of correlation	0.0–0.2

- Calculate the factor load

$$a_{ij} = u_{ij}\sqrt{\lambda_i}\left(i = 1, 2, \cdots, p, \quad j = 1, 2, \cdots, m\right) \tag{8}$$

The factor loading matrix is obtained as follows:

$$A = \begin{bmatrix} a_{11} & a_{12} & \cdots & a_{1m} \\ a_{21} & a_{22} & \cdots & a_{2m} \\ \vdots & \vdots & \vdots & \vdots \\ a_{p1} & a_{p2} & \cdots & a_{pm} \end{bmatrix} \tag{9}$$

- Score of factor variables was calculated

Firstly, the factor variable is expressed as a linear combination of the original variables, namely:

$$F_j = \beta_{j1}x_1 + \beta_{j2}x_2 + \cdots + \beta_{1p}x_p \quad \left(j = 1, 2, \cdots, m\right) \tag{10}$$

Then the factor score was obtained by regression method.

5.3. Data analysis and discussion

Twelve samples in the study area were analyzed, and two factors with eigenvalues greater than 1 were selected as the main factors. The variance contribution rate of the first major factor was 61.671%, and the cumulative variance contribution rate of the second major factor was 85.302%. Table 2 is the correlation coefficient matrix, Table 3 is the eigenvalue and cumulative variance contribution rate of the correlation matrix R, and Table 4 is the factor load matrix obtained after the rotation of the maximal variance method [9].

The variance contribution rate of the first major factor F1 is 61.671%, which is mainly composed of Mg^{2+}, TDS, SO4^{2-}, Ca^{2+}, Cl^- and other components,moreover, Mg^{2+} and SO_4^{2-} are strongly correlated with TDS, there is a strong correlation between Cl^- and TDS, a moderate correlation between Ca^{2+} and TDS, and a strong correlation between Mg^{2+} and SO_4^{2-}, indicating that Mg^{2+} and SO_4^{2-} have roughly the same source. Yellow River irrigation is the main replenish source of shallow pore water in this area, and the hydrochemical type of the Yellow River water is SO_4·HCO_3·Cl-Na·Ca·Mg. Due to the shallow buried depth of the shallow pore water in this area, the Yellow River water quickly mixed with

Table 2
Correlation coefficient of salt water chemical composition

Correlation coefficient	Na	Ca	Mg	Cl	SO_4	HCO_3	TDS
Na	1.000	–0.009	0.545	0.583	0.673	0.702	0.799
Ca	–0.009	1.000	0.711	0.330	0.608	–0.225	0.565
Mg	0.545	0.711	1.000	0.714	0.869	0.046	0.923
Cl	0.583	0.330	0.714	1.000	0.443	–0.010	0.733
SO_4	0.673	0.608	0.869	0.443	1.000	0.332	0.908
HCO_3	0.702	–0.225	0.046	–0.010	0.332	1.000	0.358
TDS	0.799	0.565	0.923	0.733	0.908	0.358	1.000

Table 3
Eigenvalues and cumulative variance contribution rates of the correlation matrix R

Serial number	Eigenvalue	Variance contribution %	Cumulative contribution rate %
1	4.317	61.671	61.671
2	1.654	23.631	85.302
3	0.749	10.696	95.998
4	0.210	3.007	99.005
5	0.052	0.742	99.747
6	0.016	0.235	99.982
7	0.001	0.018	100.000

Table 4
Maximum variance method rotation factor load matrix

Project	1	2
Na	0.488	0.849
Ca	0.803	–0.397
Mg	0.976	0.090
Cl	0.729	0.171
SO_4	0.851	0.340
HCO_3	–0.024	0.922
TDS	0.908	0.415

groundwater after brief infiltration after irrigation, and the groundwater was dominated by Mg^{2+}, Ca^{2+}, SO_4^{2-}, Cl^- and other components. It can be seen that mixing is the main factor affecting the chemical composition of groundwater in this area.

The variance contribution rate of the second main factor, F2, was 23.631%. F2 was mainly composed of HCO_3^- and Na^+, and there was a strong correlation between HCO_3^- and Na^+. In this area, the buried depth of water level is relatively shallow, evaporation and concentration is strong, runoff is slow, hydrodynamic conditions are poor, and water cycle alternation is weak, which makes the salinity increase continuously, Ca^{2+}, Mg^{2+} and SO_4^{2-} plasma reach saturation in water one after another and precipitate out, making the groundwater mainly HCO_3^- and Na^+. The main factor F2 reflects the influence of evaporation and concentration on groundwater [10–17].

6. Conclusions

Based on the study of the hydrogeological conditions in the north region, the hydrogeological characteristics and hydrochemical characteristics of shallow salt water are analyzed in detail, and the main influencing factors of hydrochemical field of shallow salt water are identified by factor analysis method, and the conclusions are drawn as follows: The study area is located in the alluvial plain of the Yellow River. The shallow pore water is the main type of groundwater. The shallow saline water in the study area is distributed in the runoff area of groundwater, and the hydrochemical type is more complex. Factor analysis method can effectively identify the main factors causing the shallow brackish water field, its explained 85.302% of the shallow brackish water chemical data in the study area, in combination with characteristics of local hydrogeological conditions and water chemical types, it is concluded that shallow salt-water formation has experienced strong mixing action in the process of evaporation and concentration, and given priority to with mixing action.

References

[1] L. Guo, G. Zhang, X. Feng, W. Wang, Z. Li, B. Wu, Study on groundwater pollution status in Jiyuan basin and groundwater treatment technology for paper mills, Paper Asia, 2 (2019) 100–104.
[2] D. Li, S. Gan, J. Li, Z. Dong, C. Lu, Hydrochemical characteristics and formation mechanism of strontium-rich groundwater in Shijiazhuang, North China Plain, J. Chem., 2021 (2021) 1–10.
[3] G.Q. Liu, L.W. Zhu, Y.X. Sun, Hydrochemical Characteristics and Origins of Salt Groundwater in the Lower Reaches of Dagu River, Periodical of Ocean University of China, 2019.
[4] R. Prasad, K.D. Yadav, Use of response surface methodology and artificial neural network approach for methylene blue removal by adsorption onto water hyacinth, Water Conserv. Manage., 4 (2020) 79–85.
[5] S. Chacko, J. Kurian, C. Ravichandran, S.M. Vairavel, K. Kumar, An assessment of water yield ecosystem services in Periyar Tiger Reserve, Southern Western Ghats of India, Geol. Ecol. Landscapes, 5 (2021) 32–39.
[6] M. Sahana, S. Rehman, A.K. Paul, H. Sajjad, Assessing socio-economic vulnerability to climate change-induced disasters: evidence from Sundarban Biosphere Reserve, India, Geol. Ecol. Landscapes, 5 (2021) 40–52.
[7] S.M. Al-Gorany, S.Z. Al-Abachi, A.I. Arif, E.E. Aboglida, E.H. Al-Abdeli, Preliminary phytochemical screening and GC-MS analysis of bioactive constituents in the ethanolic extract of empty fruit bunches, J. Clean WAS, 4 (2020) 70–74.
[8] S. Malik, S. Mumtaz, S. Akhtar, I. Zahoor, S. Kanwal, M. Habib, M.A.H. Hashmi, M.S. Majid, Issues in Environmental Protection

Agency and recommendations to solve the problems, Environ. Ecosyst. Sci., 5 (2021) 10–14.
[9] R. Karn, A. Paudel, S. Pandey, *Hypena opulenta*: a biological weed control agent for controlling an invasive weed species, swallow-wort: a review, Environ. Contam. Rev., 3 (2020) 1–3.
[10] M.A. Seelro, M.U. Ansari, S. Manzoor A, A.M. Abodif, A. Sadaf, Comparative study of ground and surface water quality assessment using water quality index (WQI) in Model Colony Malir, Karachi, Pakistan, Environ. Contam. Rev., 3 (2020) 4–12.
[11] J. Liu, M. Wang, Z. Gao, Q. Chen, F. Li, Hydrochemical characteristics and water quality assessment of groundwater in the Yishu River Basin, Acta Geophys., 68 (2020) 877–889.
[12] B. Zya, C. Ql, A. Jw, B. Sx, A. Jw, Identification of the long-term variations of groundwater and their governing factors based on hydrochemical and isotopic data in a river basin, J. Hydrol., 592 (2020) 125604, doi: 10.1016/j.jhydrol.2020.125604.
[13] J. Zhang, Y. Lai, J. Li, Y. Zhao, Study on the influence of hydro-thermal-salt-mechanical interaction in saturated frozen sulfate saline soil based on crystallization kinetics, Int. J. Heat Mass Transfer, 146 (2020) 118868, doi: 10.1016/j.ijheatmasstransfer.2019.118868.
[14] H.T. Hoang, R. Baeumle, Complex hydrochemical characteristics of the Middle-Upper Pleistocene Aquifer in Soc Trang Province, Southern Vietnam, Environ. Geochem. Health, 41 (2019) 325–341.
[15] P. Bujard, Interference Pigments on the Basis of Perlite Flakes, WO, 2019.
[16] C. Zhang, L. Chen, H. Si, W. Gao, P. Liu, J. Zhang, Study on the characteristics and mechanisms of nicosulfuron biodegradation by *Bacillus velezensis* CF57, J. Basic Microbiol., 60 (2020) 649–658.
[17] Y. Jia, K. Bian, C. Li, X. Bai, F. Bai, Analysis of hydrochemical characteristics of Karstic water in Fengfeng Mining area based on GIS and correlation, China Coal, 6 (2019) 134–139.